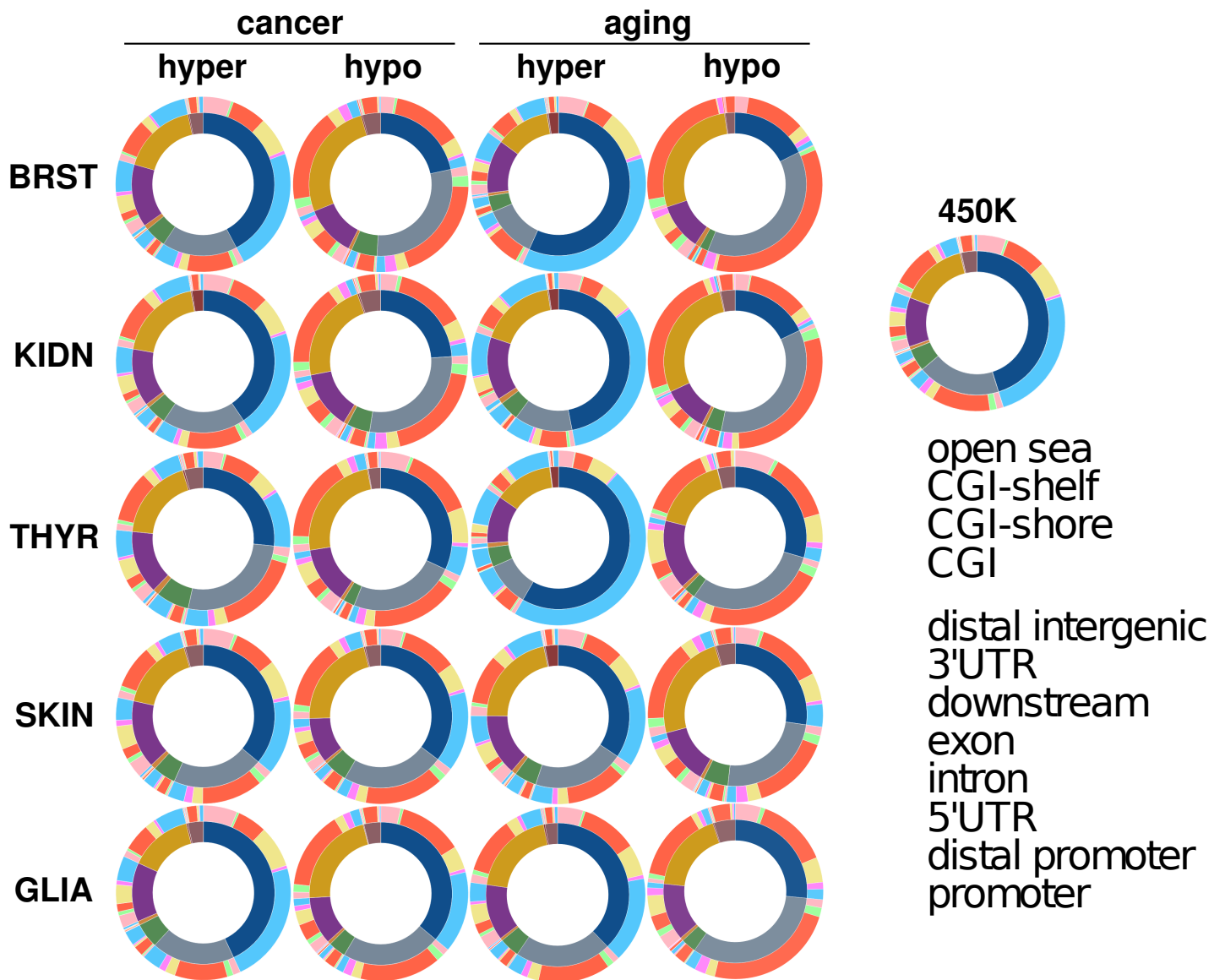
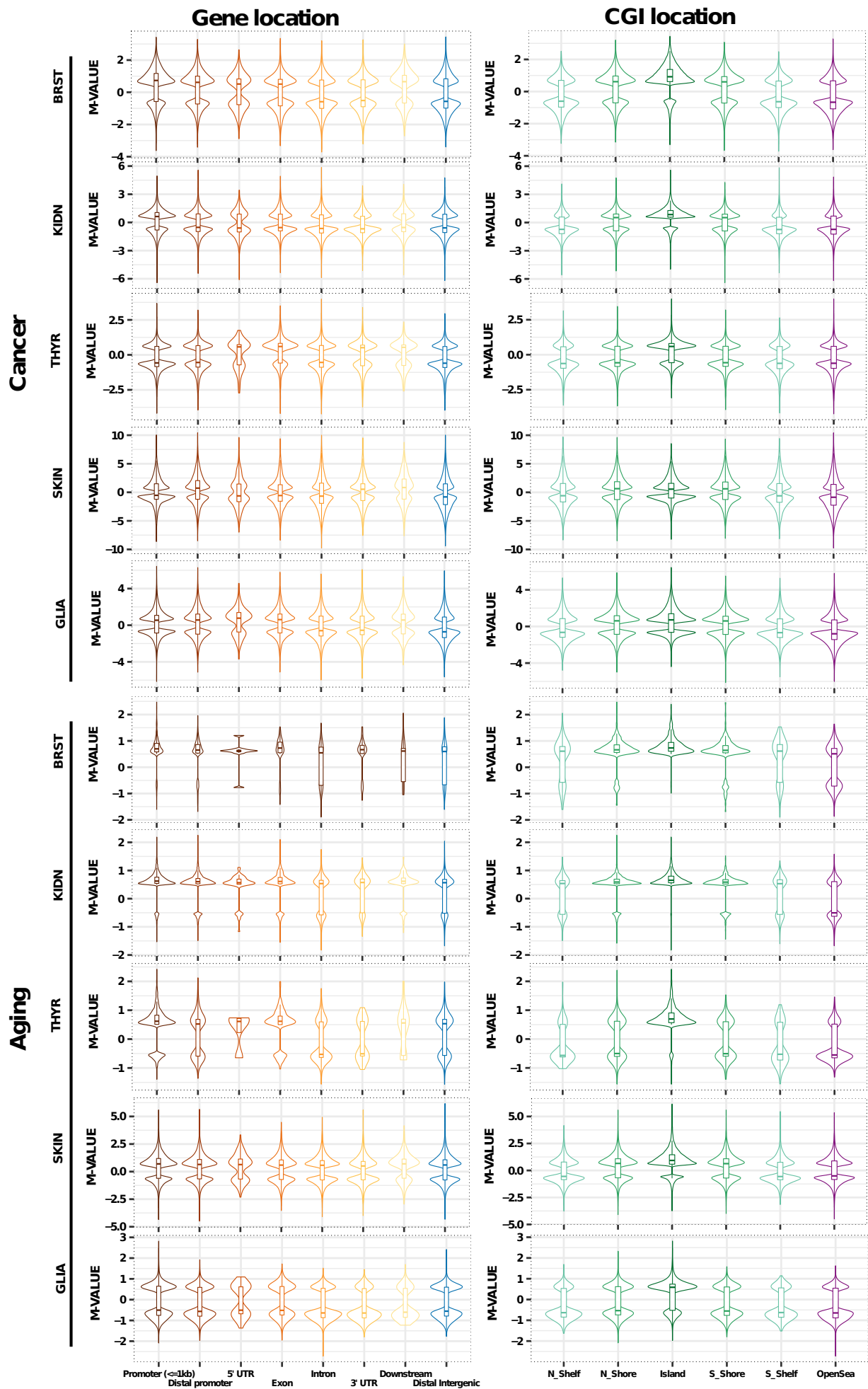


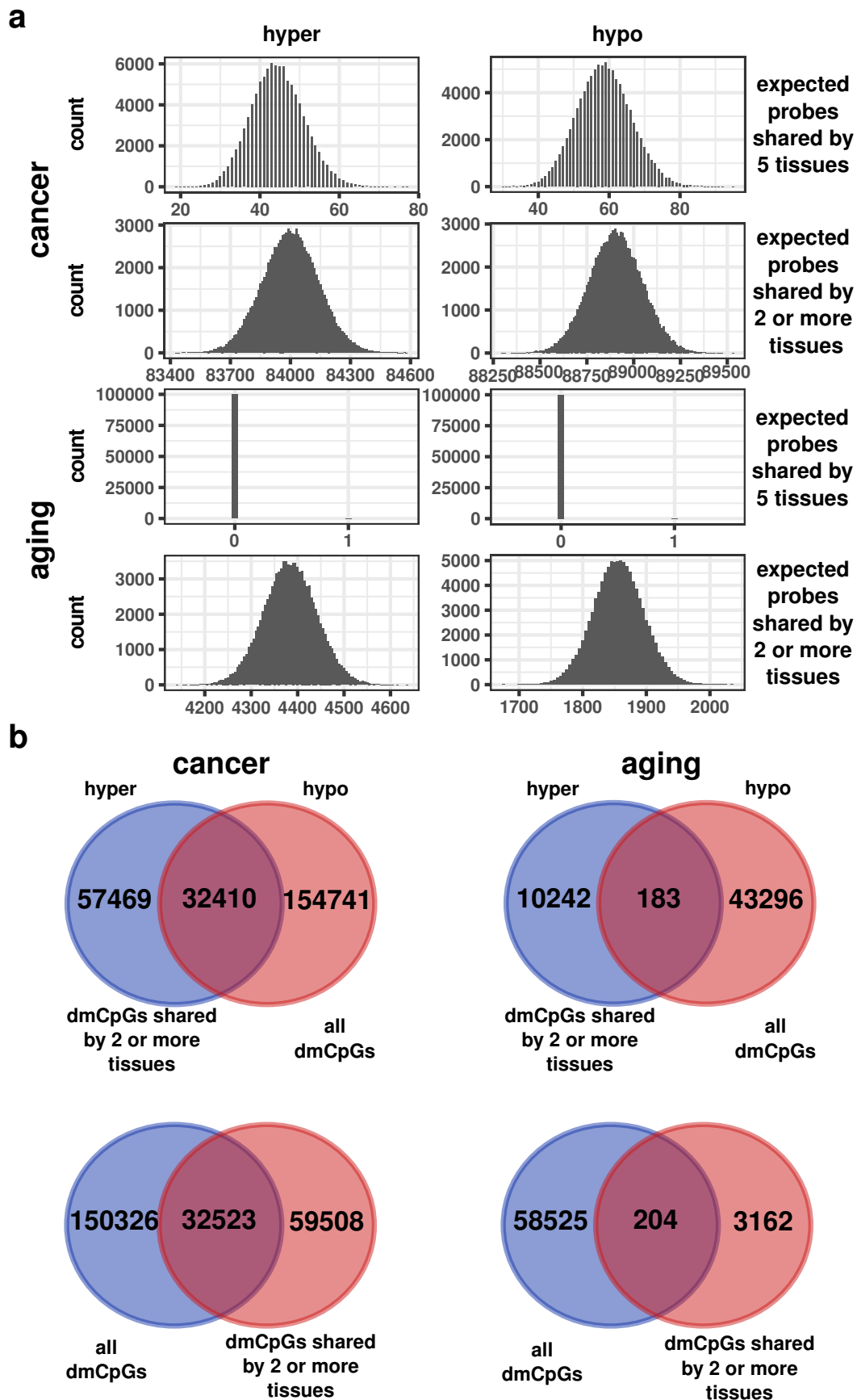
**Figure S1. Hierarchical clustering and heatmaps including the 1,000 most significant dmCpGs for cancer and aging analyses. Methylation values are displayed from zero (green) to one (red).**



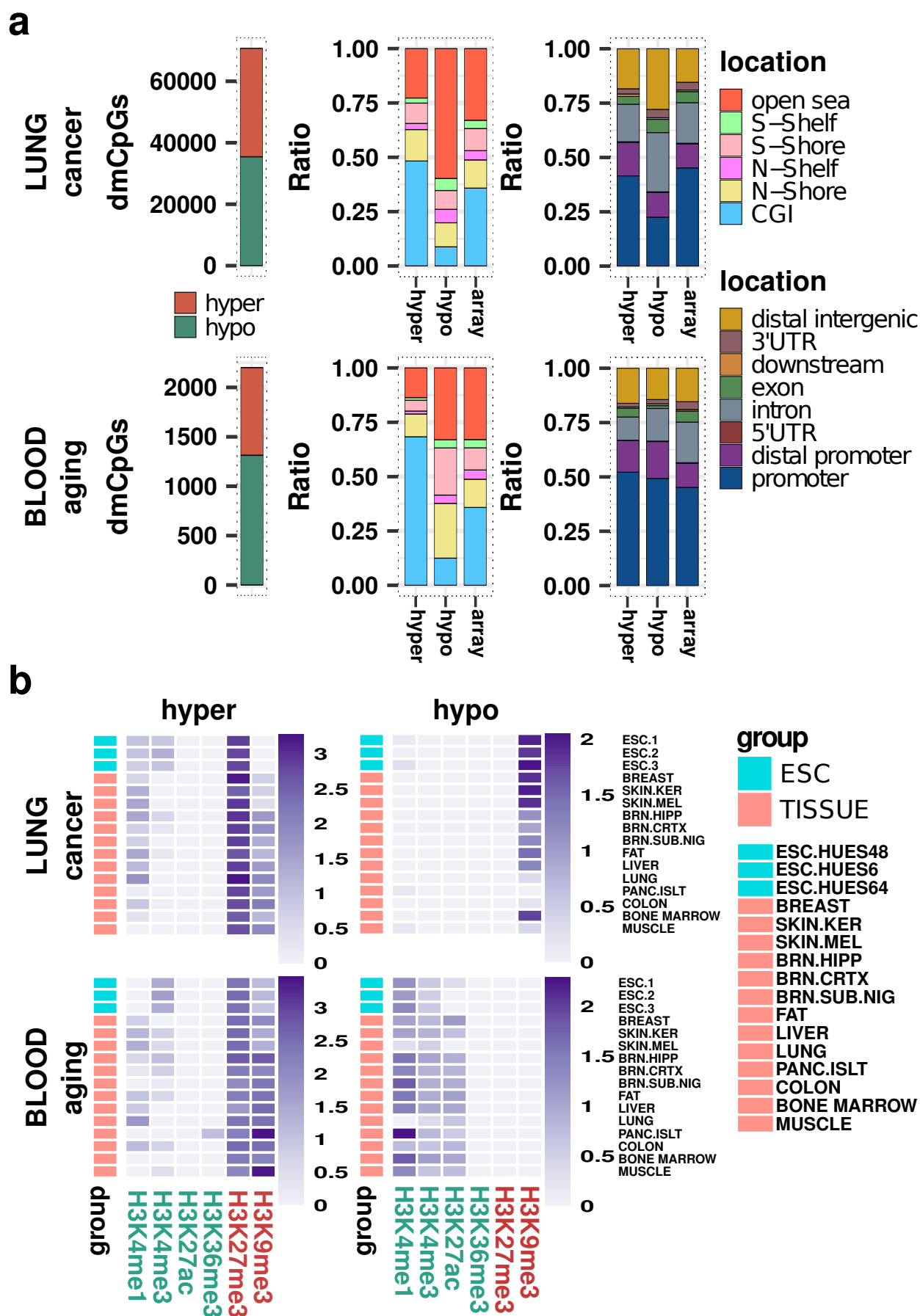
**Figure S2. Sunburst plot charts representing integrated information of relative distribution of differentially methylated CpG according to their CpG island status (outer circle) and gene location status (inner circle).**



**Figure S3. Violin plots representing magnitude of M-value methylation changes in cancer and aging, according to CpG island status (right plots) and gene location (left plots).**

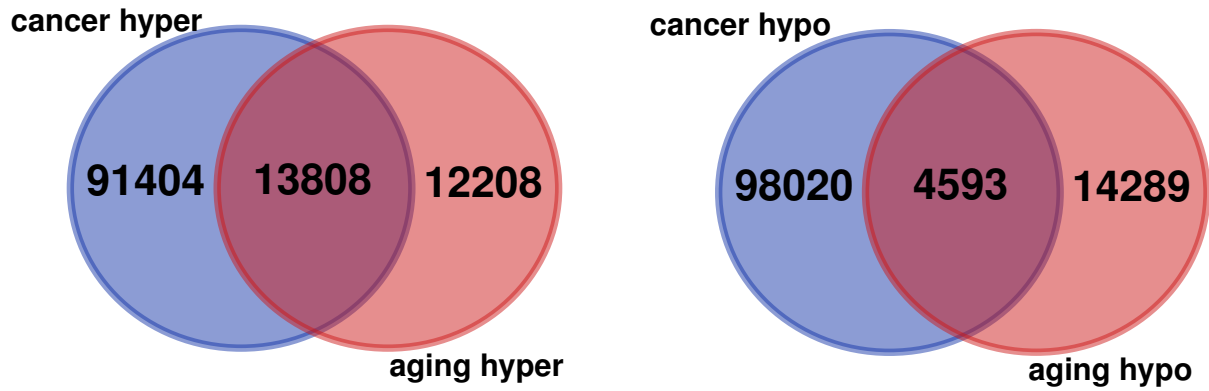


**Figure S4. a** Histograms showing obtained overlaps from 105 simulations of randomly extracting 5 sets of probes of sizes equal to the obtained dmCpGs of cancer and aging. **b** Overlap of hyper- and hypomethylated dmCpGs in aging and cancer. Venn diagrams showing the number and overlap total of non-redundant hyper- and hypomethylated dmCpGs detected in cancer and aging, when selecting dmCpGs shared by two or more tissues. Cancer Hyper Shared vs Hypo All: Fisher's test  $P < 0.001$ , OR = 0.43, Expected hypergeometric mean, EHM = 46,506, Jaccard Index, JI = 0.13. Cancer Hypo Shared vs Hyper All: Fisher's Test  $P < 0.001$ , OR = 0.43, EHM = 46,525, JI = 0.13. Aging Hyper Shared vs Hypo All: Fisher's Test  $P < 0.001$ , OR = 0.13, EHM = 1,253, JI = 0.003. Aging Hypo Shared vs Hyper All: Fisher's Test  $P < 0.001$ , OR = 0.33, EHM = 547, JI = 0.003.

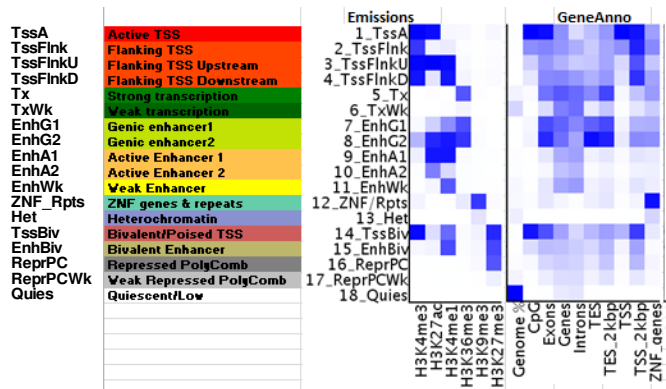


**Figure S5. Additional lung and whole blood dataset analysis. a** From left to right: stacked barplots indicating total number of dmCpGs detected in lung cancer and blood aging; stacked barplots indicating relative distribution of differentially methylated CpGs according to their CpG island status; stacked barplots indicating relative distribution of differentially methylated CpGs according to their gene location status. **b** Heatmaps depicting significant ( $P < 0.05$ ) over-enrichment of hyper- and hypomethylated dmCpG sites with different histone marks in aging and cancer, in a selection of 16 cell- and tissue-types (see Additional file 9: Table S8 for 98 full cell and tissue-types). Color code indicates the significant enrichment based on  $\log_2$  odds ratio (OR).

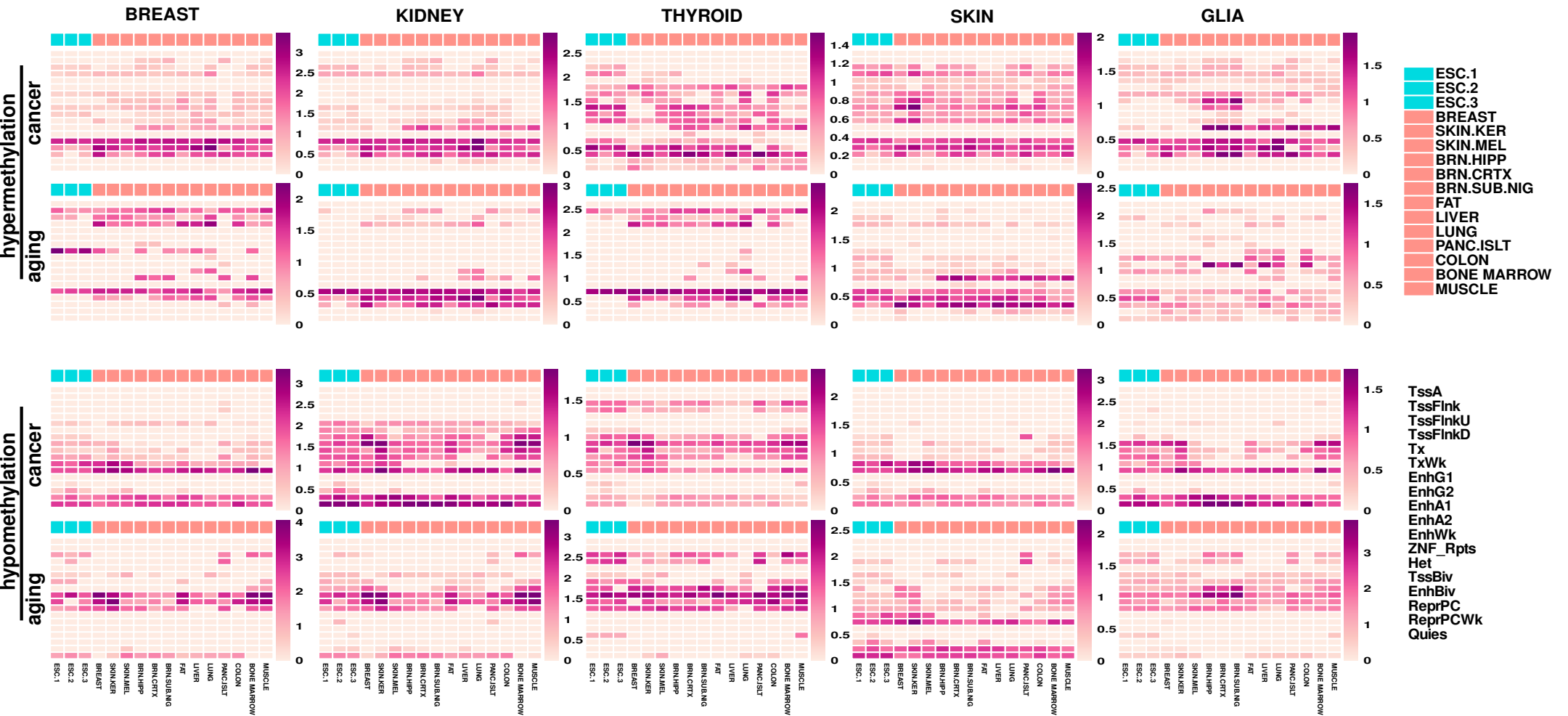
## no skin



**Figure S6.** Venn diagrams showing the number and overlap of total non-redundant hyper- (left) and hypomethylated (right) dmCpGs detected in cancer and aging, without taking SKIN tissue into account. dmCpGs that were only hypermethylated or only hypomethylated between all tissues were chosen for the comparison. Fisher's tests, both  $P < 0.001$ , ORs = 3.0 and 0.8, expected hypergeometric means = 7,568 and 5,357; JI = 0.12 and 0.05, respectively.



**Figure S7. Heatmaps showing significant ( $P < 0.05$ ) over-enrichment of hyper- and hypomethylated dmCpG sites with different chromatin states in aging and cancer, in a selection of 16 cell- and tissue types (see Additional file 11: Table S10 for 98 full cell- and tissue-types). Color code indicates the significant enrichment based on log2 odds ratio (OR). On top of the figure, the NIH Roadmap learned ChromHMM model is displayed.**



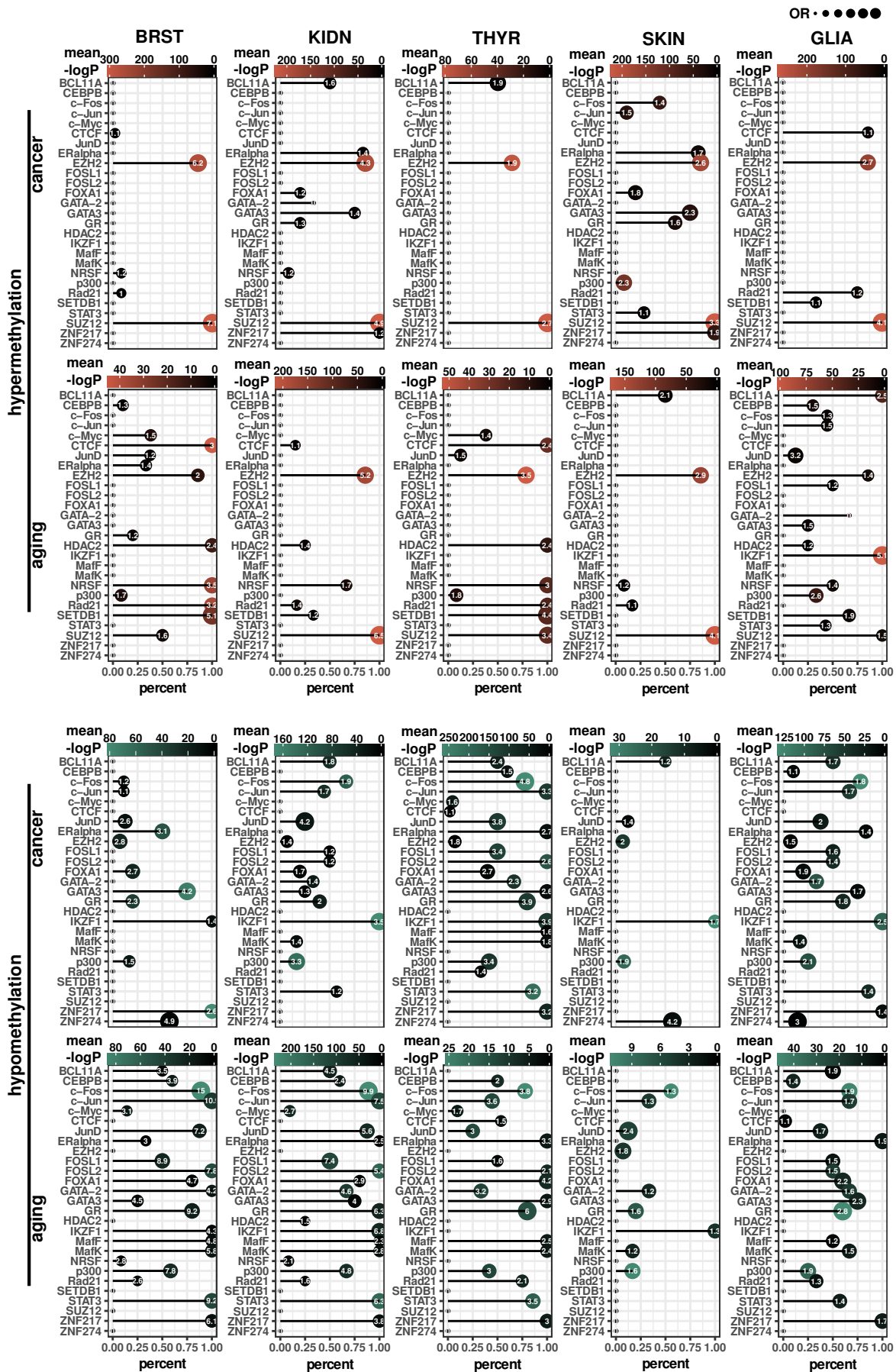


**Figure S8. Lollipop plots showing the enrichment of different transcription factors at hyper- and hypomethylated dmCpG sites in aging and cancer. Color code indicates the significance of the over-enrichment based on log10 P-value. Sizes of circles and their corresponding numbers indicate enrichment based on odds ratio (OR). X-axis measures the percentage of possible tracks for which a significant enrichment was detected, as this is also a measure of enrichment. Only the most representative transcription factors (those that appeared as significantly over-enriched in at least 3 tracks or with an OR>3 in any track) were selected for data representation.**



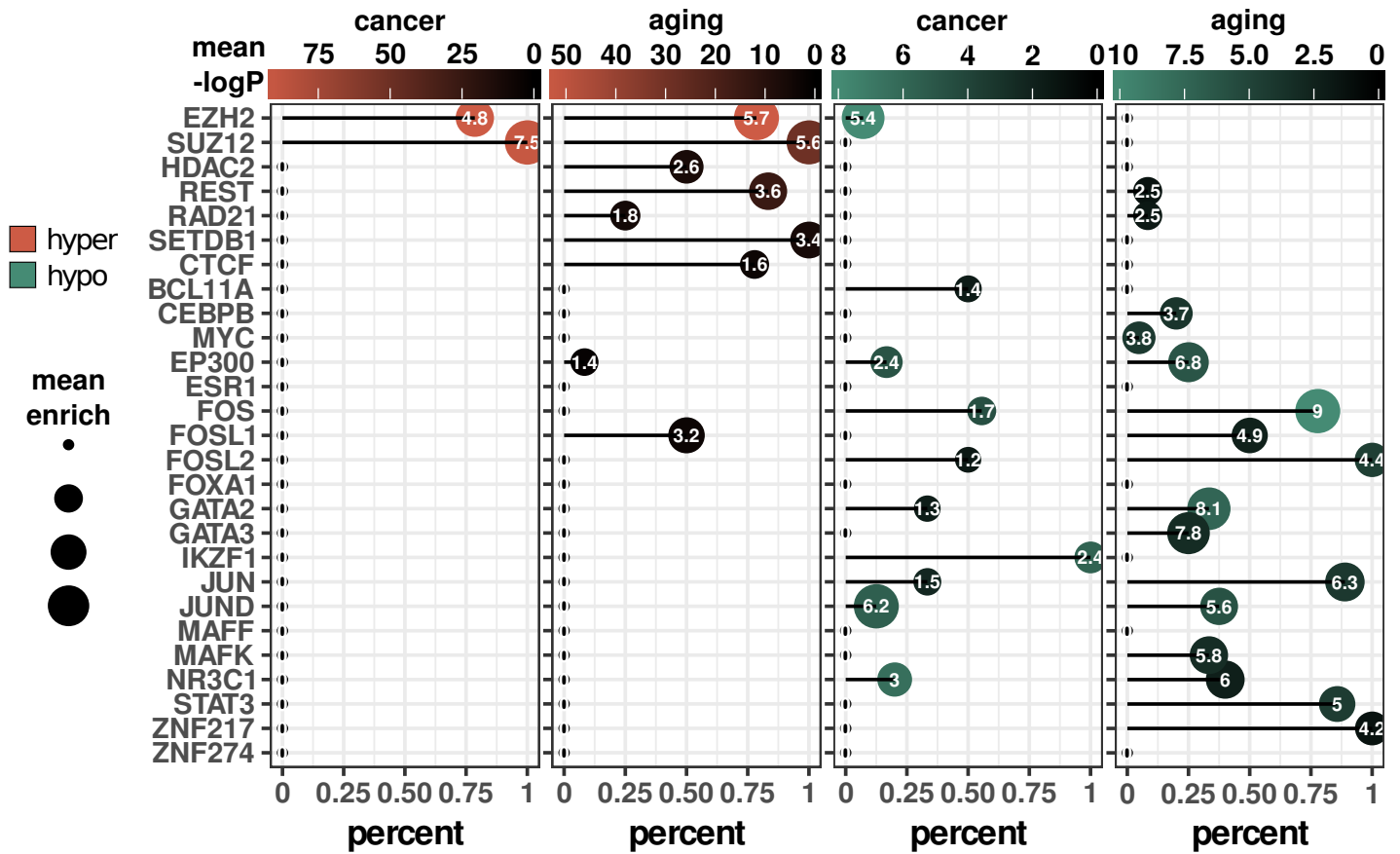
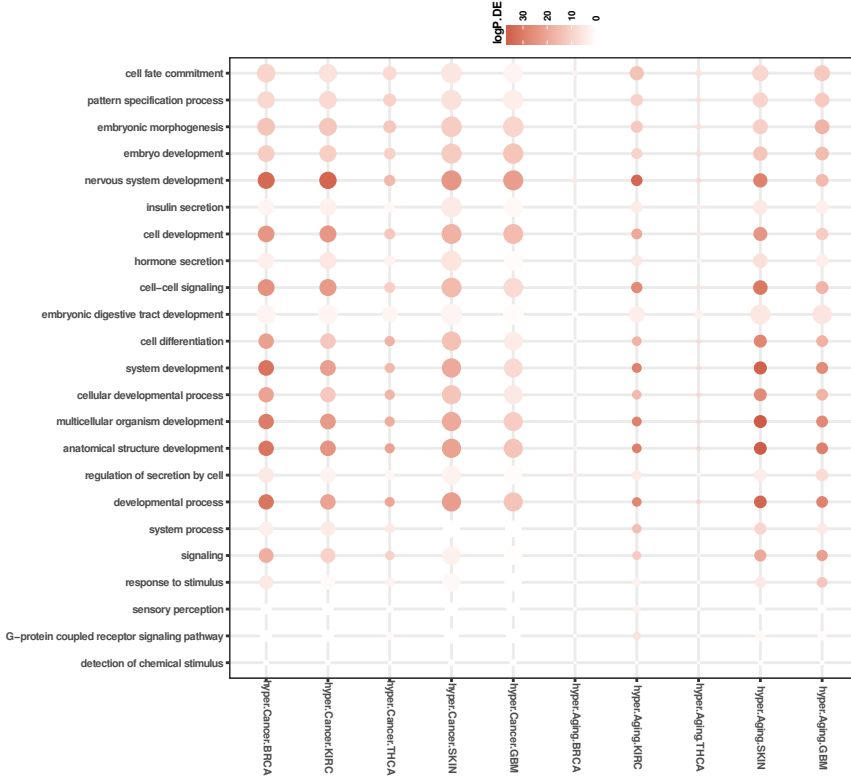
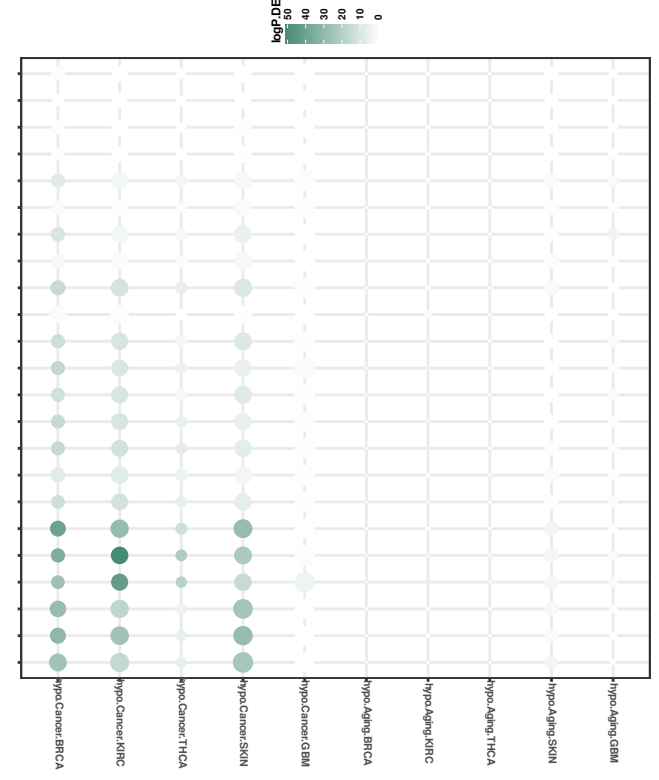


**Figure S9. Lollipop plots showing the enrichment of different transcription factors for common hyper- and hypomethylated dmCpGs shared between 5 tissues for cancer (1,962 and 2,708 probes, respectively) or 3 tissues for aging (904 and 106 probes, respectively) (see Additional file 7: Table S6 for CpG lists). Color code indicates the significance of the over-enrichment based on log<sub>10</sub> P-value. Sizes of circles and their corresponding number indicate enrichment based on odds ratio (OR). X-axis measures the percentage of possible tracks for which a significant enrichment was detected, as this is also a measure of enrichment.**

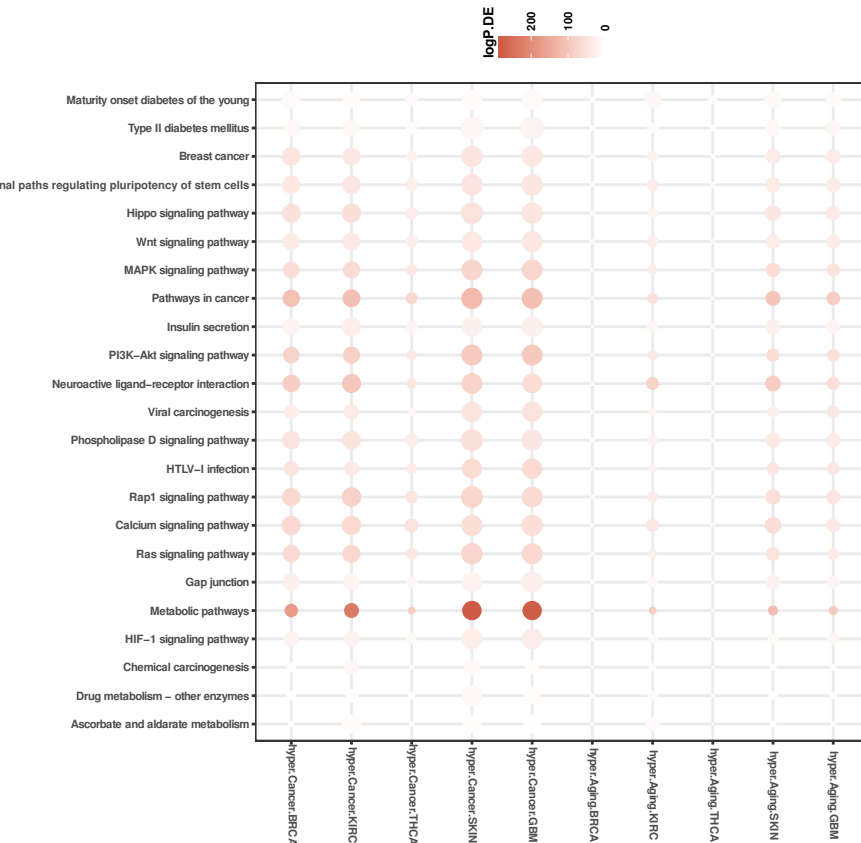
### Cancer hypermethylation ontologies



### Cancer hypomethylation ontologies



### Aging hypermethylation ontologies



### Aging hypomethylation ontologies

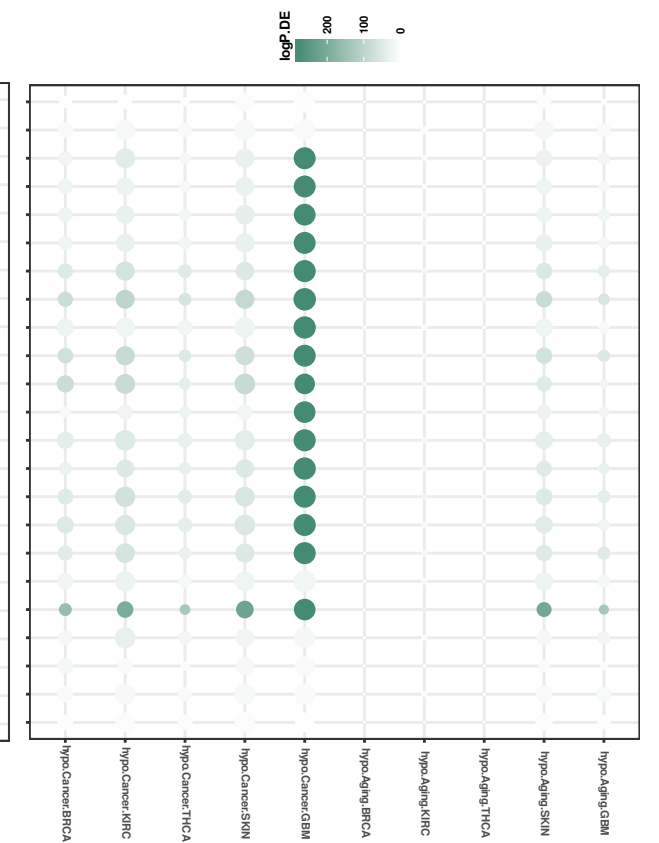
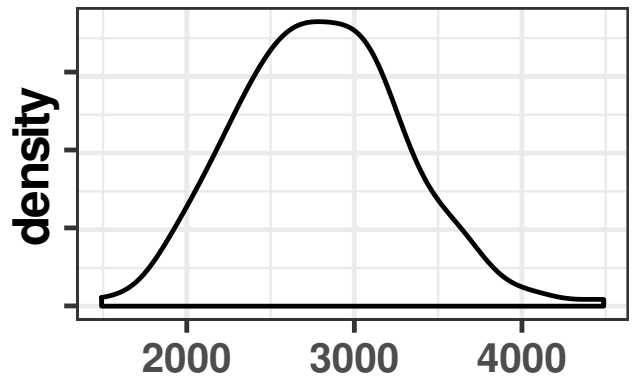
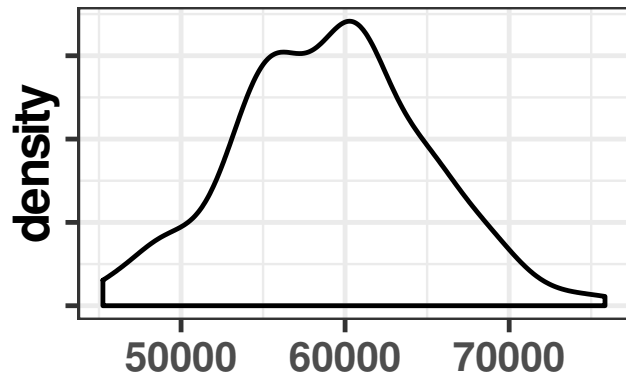


**Figure S10. Panels indicating gene and KEGG pathway ontology enrichment for hyper- and hypomethylation dmCpGs in aging and cancer (see Additional file 13: Table S12 for detailed information).**



total  $>|\pm 0.9|$  correlations



total  $>|\pm 0.8|$  correlations

percentage of total possible correlations

	$> \pm 0.9 $	$> \pm 0.8 $
random	0.015%	0.306%
aging	0.026%	0.521%
cancer	0.025%	0.495%

Figure S11. Density plots showing the number of Spearman correlations observed between DNA methylation and gene expression ( $> 0.8$  or  $< -0.8$ ) generated by randomly extracting 150 sets of 1000 probes from the KIRC 450K array and computing the correlations against all the genes expressed in the KIRC dataset across 18 normal kidney samples. On the right, the percentages of  $>|\pm 0.8|$  correlations as compared to the total number of the computed correlations is shown.